ChemComm

Chemical Communications

www.rsc.org/chemcomm

Number 43 | 21 November 2008 | Pages 5441–5652

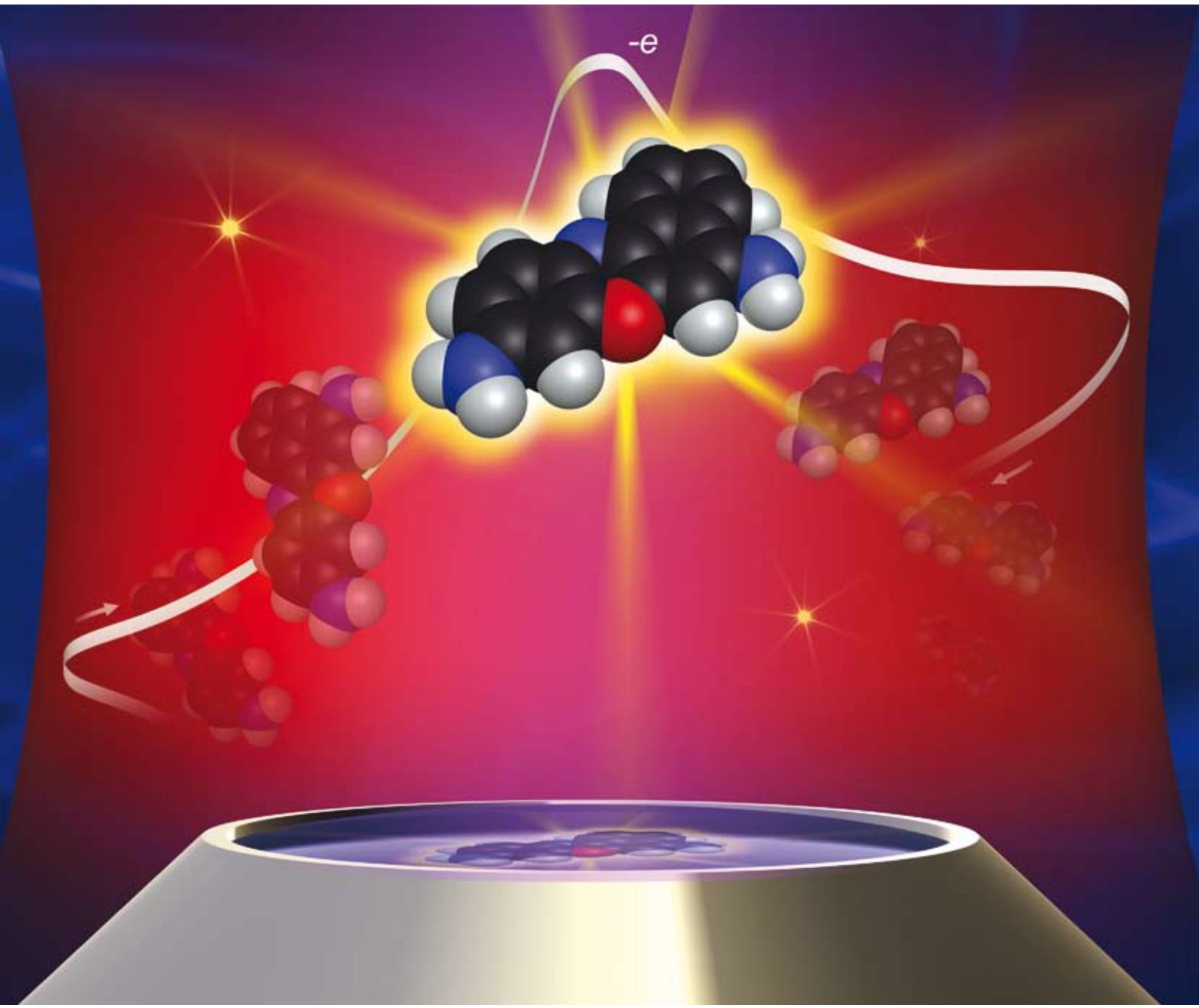

ISSN 1359-7345

RSC Publishing

1359-7345(2008)43;1-Y

Single-molecule fluorescence spectroelectrochemistry of cresyl violet

Chenghong Lei,† Dehong Hu† and Eric J. Ackerman*

Received (in Cambridge, UK) 16th July 2008, Accepted 22nd August 2008
First published as an Advance Article on the web 12th September 2008
DOI: 10.1039/b812161c

Here we report a new path to study single molecule electron transfer dynamics by coupling scanning fluorescence microscopy with a potentiostat *via* a conventional electrochemical cell to enable single-molecule fluorescence spectroelectrochemistry of cresyl violet in aqueous solution, demonstrating that the single-molecule fluorescence intensity of cresyl violet is modulated synchronously with the cyclic voltammetric potential scanning.

The dynamics of electron transfer processes have been studied using ensemble-averaging approaches.[1–4] However, molecular inhomogeneities make it highly difficult for ensemble-averaged measurements to dissect complex electron transfer mechanisms. Consequently, these measurements sometimes produced inconsistent experimental results, such as the large difference in measured electron transfer rate constants.[5] The inconsistencies stem from both spatial and temporal inhomogeneities, which can be identified, measured, and analyzed by studying one molecule at a time.[6] Single-molecule spectroscopy has been demonstrated to be a powerful approach for studying complex systems and inhomogeneous dynamics and has also been applied to intramolecular and interfacial electron transfer investigations.[7–11] By combining single-molecule spectroscopy and electrochemistry, single oxidation/reduction events can be measurable. Single-molecule spectroelectrochemistry of a conjugated polymer in acetonitrile solution has been reported.[12]

Cation dyes of phenazines, phenoxazines and phenothiazines have been extensively used as electron transfer mediators for enzymatic reactions and biosensor development.[13–16] Among these electroactive cation dyes, cresyl violet is very attractive because it is also strongly fluorescent.[17] The high fluorescence quantum efficiencies of cresyl violet ($\sim$0.5) enable its use in single-molecule fluorescence spectroscopy to study electron transfer processes.[18] In this work, we develop cyclic voltammetry-coupled single-molecule fluorescence spectroscopy using cresyl violet as a model fluorescent redox molecular probe to investigate the electron transfer dynamics of single redox molecules in aqueous solution. A sample-scanning confocal fluorescence microscope was synchronized with a potentiostat that allows cresyl violet to be oxidized and reduced by cyclic voltammetric potential scanning. The potentiostat was connected to a conventional electrochemical cell equipped with a three-electrode system using a transparent indium tin oxide (ITO)/glass cover slip as the working electrode (Fig. 1). The aqueous working solution contained 1.2 nM cresyl violet, a concentration where there is on average less than one molecule in the laser focal volume, thereby avoiding interference from molecular aggregation. Single-molecule fluorescence intensity changes were modulated by cyclic voltammetric potential scanning. We attribute the single-molecule fluorescence change to the redox reaction of single molecules.

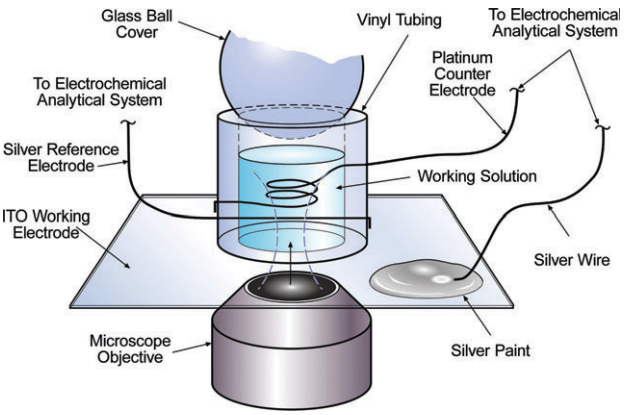

Fig. 1 Schematic of an electrochemical cell coupled with scanning confocal fluorescence microscopy.

In this work,‡ we first studied the cyclic voltammetry of a 36 μM cresyl violet solution with a standard electrochemical reactor using a glassy carbon electrode. Cresyl violet underwent quasi-reversible reduction/oxidation reaction in aqueous solution (not shown) with a formal potential of approximately −0.35 V (*vs.* Ag/AgCl). Next, single molecule fluorescence of the reduced and oxidized states of cresyl violet were studied with the combined setup of cyclic voltammetry and fluorescence microscopy (Fig. 1). The excitation laser from the fluorescence microscope was focused in the solution several microns above the ITO surface to probe the solution phase cresyl violet molecules. The cyclic voltammograms in Fig. 2A show the similar quasi-reversible redox peaks of cresyl violet at the ITO electrode (Fig. 1) to that at the carbon electrode. Fig. 2B shows the change of fluorescence intensity of the cresyl violet solution simultaneously recorded during the cyclic voltammetric measurement displayed in Fig. 2A.

Fig. 2B shows that the fluorescence intensity level increases and decreases with respect to ramping up and down the voltage. This result suggests that the oxidized state of cresyl violet emits strong fluorescence and its reduced state yields very weak or no fluorescence. The reaction is proposed as:

$$\text{Cresyl violet (non-fluorescent)} \underset{+e^-}{\overset{-e^-}{\rightleftharpoons}} \text{Cresyl violet}^+\text{(fluorescent)} \quad (1)$$

Pacific Northwest National Laboratory, Richland, Washington 99352, USA. E-mail: Chenghong.Lei@pnl.gov. E-mail: Dehong.Hu@pnl.gov. E-mail: Eric.Ackerman@pnl.gov; Fax: +1 509 3766767
† These authors contributed equally to this work.

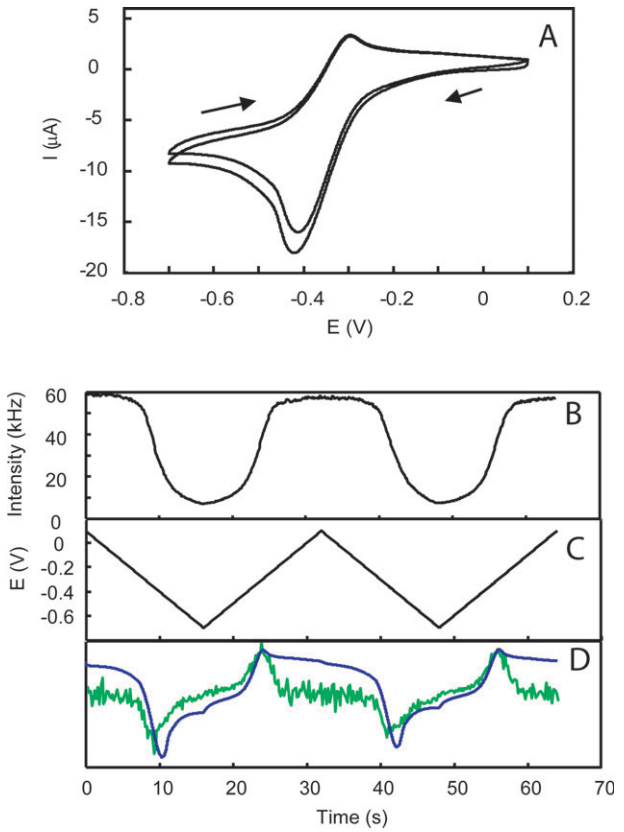

Fig. 2 Ensemble averaged fluorescence spectroelectrochemistry of cresyl violet: (A) cyclic voltammograms of 36 μM cresyl violet in pH 6.2, 20 mM sodium phosphate at the ITO electrode. Scan rate: 50 mV s^{-1}; (B) plot of fluorescence intensity of the cresyl violet solution *vs.* time, synchronously with the CV scanning; (C) plot of the CV potential *vs.* time; (D) time derivative of fluorescence intensity of the cresyl violet solution during the CV scanning (green curve) and plot of the CV current *vs.* time (blue curve).

To further illustrate the relationship between the electrochemical and the fluorescence measurements, we plotted the cyclic voltammetry data in the time domain, voltage *vs.* time (Fig. 2C) and current *vs.* time (Fig. 2D, blue curve) so they can be overlaid with fluorescence on the same axis. The green line of Fig. 2D is the derivative of the fluorescence intensity displayed in Fig. 2B, which follows the current as they both represent the rate of reaction d[cresyl violet$^+$]/dt (Fig. 2D). Since the current signal contains other factors, such as charging double layer, the two curves do not overlap completely. A single molecule signal would be dependent on other factors as well; *e.g.* dye molecules could be strongly oriented by the electric field forming at the electrode surface; or the dye's fluorescence quantum yield could be dependent upon its local environment such as ionic strength or pH at the electrode surface at certain potentials.

The fluorescence intensity levels at high and low potentials show a ratio of high to low intensity of ~8 : 1 (Fig. 2B). Two potential explanations are: (a) all molecules are reduced/oxidized at the lowest/highest potentials and the reduced state exhibits ~8 times weaker fluorescence; or (b) the reduced state has no fluorescence but ~1 out of 8 cresyl violet molecules remains in the oxidized state even at the lowest potential (as shown in the equation). It is difficult to differentiate between these two possibilities using only the ensemble averaged experimental data (Fig. 2).

To differentiate between the two cases, we conducted cyclic voltammetry with single molecule fluorescence experiments by lowering cresyl violet concentration significantly. With 200 μW excitation focused in a 1.2 nM cresyl violet solution, single molecules can be detected. Because the solution is very dilute, there is less than one molecule in the laser focal volume on average. Single molecules diffuse in and out of the laser excitation volume randomly. Once a molecule enters the excitation volume, a fluorescence burst is detected. Although the fluorescence bursts have a broad intensity distribution due to the randomness of diffusion, the data for burst time, intensity and width were analyzed extensively for the physical and chemical properties of single molecules.[19] We observed tens of thousands of fluorescence bursts during 3 cycles of CV scans over a 50 s window. Unlike the ensemble experiments (Fig. 2A), the redox reactions of cresyl violet single molecules were not detectable by CV alone (Fig. 3A) because of the 30 000-fold lower concentration of the dye. Nonetheless, the single molecule fluorescence burst data (Fig. 3C and D) clearly reflect the effect of CV scanning (Fig. 3B).

In this experiment, 48 s were used for 3 CV cycles and the remaining 2 s were recorded without CV scanning. The fluorescence trajectory of cresyl violet was synchronously

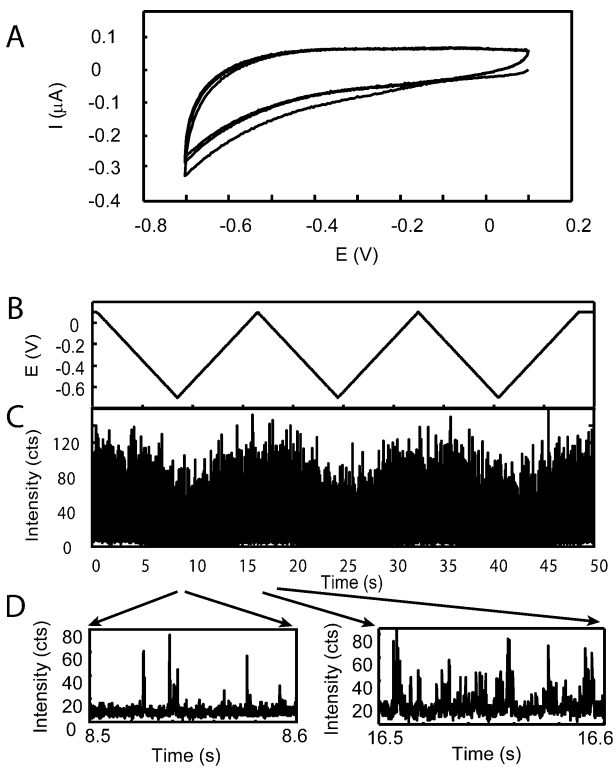

Fig. 3 Single-molecule fluorescence spectroelectrochemistry of cresyl violet: (A) cyclic voltammograms of 1.2 nM cresyl violet in pH 6.2, 20 mM sodium phosphate at the ITO electrode. Scan rate: 100 mV s^{-1}; (B) potential *vs.* time plot of the CV scan; (C) single-molecule fluorescence intensity burst trajectory of cresyl violet *vs.* time. The bin time of the time trajectory is 0.1 ms; (D) two 0.1 s segments of the fluorescence time trajectory.

modulated with recorded cyclic voltammetric potential (Fig. 3B–D). We chose two points in this CV scan as typical examples, the time window between 8.5 and 8.6 s corresponding to the lowest potential, −0.7 V on the working electrode, and the time window between 16.5 and 16.6 s corresponding to the highest potential, 0.1 V on the working electrode. The time window 16.5–16.6 s exhibits much more fluorescence bursts than the time window 8.5–8.6 s (Fig. 3D). Therefore, high potential is related to higher burst density and *vice versa* (Fig. 3C and D). Importantly, these single molecule burst data provide clues to differentiate the two potential explanations for the ensemble experiments. For case (a), if both strongly fluorescent oxidized cresyl violet and weakly fluorescent reduced cresyl violet single molecules were counted, the number of bursts per time window would not change with the potential while the burst size would change with the potential. For case (b), if reduced cresyl violet has no fluorescence and is not counted, a change in the number of bursts per time window with respect to the potential would occur. The experimental results in Fig. 3 indeed demonstrate a dramatic change in the number of bursts. Therefore, case (b) is more suitable to describe the redox reaction of cresyl violet. Because the number of bursts per unit time is proportional to the local concentration of the fluorescent species, the data is consistent with only a small fraction of cresyl violet molecules randomly diffusing into the laser excitation volume remaining in the oxidized state even at the lowest potential. This also explains why the ensemble experiments show some fluorescence intensity even at the lowest potential (−0.7 V) (Fig. 2B), although the local concentration of the fluorescent species was modulated by the electrochemical potential and the majority of the strongly fluorescent oxidized form of cresyl violet was converted to the non-fluorescent reduced form when the potential was low (< -0.45 V).

In summary, we demonstrated single molecule fluorescence spectroscopy coupled with cyclic voltammetry using a conventional three-electrode electrochemical method. Cyclic voltammetry-coupled single-molecule fluorescence spectroscopy can monitor single-molecule levels of a reversible or quasi-reversible redox electrochemical reaction of a molecule if the molecule is electroactive and strongly fluorescent. The results open up a new path to study single molecule electron transfer dynamics by measuring electrochemistry and single molecule fluorescence spectroscopy simultaneously.

We gratefully acknowledge funding of this work by the US Department of Energy Office of Basic Energy Sciences under Contract DE-AC06-RLO1830. A portion of the research described in this paper was performed in the Environmental Molecular Sciences Laboratory, a national scientific user facility sponsored by the Department of Energy's Office of Biological and Environmental Research and located at Pacific Northwest National Laboratory.

Notes and references

‡ All electrochemical experiments were carried out with a potentiostat (Autolab PSTAT12, Eco Chemie, Netherlands). A working buffer of pH 6.2, 5–20 mM sodium phosphate was used throughout this work. The potentiostat was connected to an electrochemical reactor (0.5 mL) equipped with a glassy carbon electrode as the working electrode, an Ag/AgCl (3.0 M NaCl) reference electrode, and a platinum wire counter electrode for the ensemble electrochemical experiments. When coupled with fluorescence single-molecule microscopy, the potentiostat was connected to a specially-designed electrochemical cell equipped with an ITO cover slip (22 × 22 mm, 8–12 Ω) as a working electrode, an Ag wire as the quasi-reference electrode, a platinum wire coil as the counter electrode (see Fig. 1). The working solution was inside 10 cm of vinyl tubing (5/16 inch OD and 3/16 inch ID) attached to the ITO surface by epoxy glue. The tube holds 120 μL of solution above an exposed ITO surface area of 12.5 mm^2. The silver wire reference electrode is ∼2 mm above and parallel to the ITO surface. The Pt wire counter electrode is ∼4 mm above the ITO surface. A glass ball was used as a cell stopper to prevent the solution from evaporating.

The experimental setup for the single-molecule fluorescence microscope was described previously.[20] Briefly, single-molecule images and fluorescence intensity trajectories were recorded using a Zeiss inverted sample-scanning confocal microscope, equipped with a 100× 1.3 NA oil immersion objective (Zeiss FLUAR), single-photon counting avalanche photodiode (APD) detector (Perkin-Elmer SPCMAQR-15), home-made photon time-stamping electronics, and scanning piezo-electric stage (Queensgate). A 594 nm HeNe laser was brought to the microscope's epi-port by a single mode optical fiber. The excitation power used for imaging was 0.4 μW when focusing on the electrode surface, and 200 μW when focusing in solution. The excitation was reflected by a dichroic mirror (Z594RDC, Chroma). The emission passed through this dichroic mirror and laser cutoff filter (HQ615LP, Chroma) prior to being detected by APD.

1 G. T. Brown, J. R. Darwent and P. D. I. Fletcher, *J. Am. Chem. Soc.*, 1985, **107**, 6446–6451.
2 K. A. Walters, D. A. Gaal and J. T. Hupp, *J. Phys. Chem. B*, 2002, **106**, 5139–5142.
3 D. Duonghong, J. Ramsden and M. Gratzel, *J. Am. Chem. Soc.*, 1982, **104**, 2977–2985.
4 J. B. Asbury, E. Hao, Y. Wang, H. N. Ghosh and T. Lian, *J. Phys. Chem. B*, 2001, **105**, 4545–4557.
5 P. F. Barbara, T. J. Meyer and M. A. Ratner, *J. Phys. Chem.*, 1996, **100**, 13148–13168.
6 N. G. Walter, C.-Y. Huang, A. J. Manzo and M. A. Sobhy, *Nat. Methods*, 2008, **5**, 475–489.
7 M. W. Holman, R. C. Liu and D. M. Adams, *J. Am. Chem. Soc.*, 2003, **125**, 12649–12654.
8 R. C. Liu, M. W. Holman, L. Zang and D. M. Adams, *J. Phys. Chem. A*, 2003, **107**, 6522–6526.
9 S. Weiss, *Science*, 1999, **283**, 1676–1683.
10 H. Yang, G. B. Luo, P. Karnchanaphanurach, T. M. Louie, I. Rech, S. Cova, L. Y. Xun and X. S. Xie, *Science*, 2003, **302**, 262–266.
11 M. Gutscher, A.-L. Pauleau, L. Marty, T. Brach, G. H. Wabnitz, Y. Samstag, A. J. Meyer and T. P. Dick, *Nat. Methods*, 2008, **5**, 553–559.
12 R. E. Palacios, F. R. F. Fan, A. J. Bard and P. F. Barbara, *J. Am. Chem. Soc.*, 2006, **128**, 9028–9029.
13 L. T. Kubota and L. Gorton, *Electroanalysis*, 1999, **11**, 719–728.
14 C. H. Lei and J. Q. Deng, *Anal. Chem.*, 1996, **68**, 3344–3349.
15 C. M. Ruan, F. Yang, C. H. Lei and J. Q. Deng, *Anal. Chem.*, 1998, **70**, 1721–1725.
16 F. Yang, C. M. Ruan, J. S. Xu, C. H. Lei and J. Q. Deng, *Fresenius' J. Anal. Chem.*, 1998, **361**, 115–118.
17 D. Magde, J. H. Brannon, T. L. Cremers and J. Olmsted, *J. Phys. Chem.*, 1979, **83**, 696–699.
18 V. Biju, M. Micic, D. Hu and H. P. Lu, *J. Am. Chem. Soc.*, 2004, **126**, 9374–9381.
19 S. M. Nie and R. N. Zare, *Annu. Rev. Biophys. Biomol. Struct.*, 1997, **26**, 567–596.
20 D. Hu and H. P. Lu, *J. Phys. Chem. B*, 2003, **107**, 618–626.

